AN ABSTRACT OF THE THESIS OF

Kimberly Hockaday Dahm for the degree of Master of Science in Chemistry presented on December 5, 1994. Title: Luminescent Properties of Inorganic Oxides

Redacted for Privacy

Abstract approved: _____

Douglas A. Keszler

The emphasis of this work has been toward characterization of the optical properties of several inorganic borates and oxoanion halides. General surveys have been conducted to identify features that may be important for the development of new phosphors.

Toward this goal, $Sr_6YAl(BO_3)_6$, a representative member of the large family of compounds designated STACK, was doped with Bi^{+3}, Pb^{+2}, Ce^{+3}, Eu^{+2}, Tb^{+3}, and Eu^{+3}. Its luminescent characteristics were predictable on the basis of the site symmetries of the Sr and Y atoms. The poor overlap between Ce emission and Tb excitation in these hosts precluded efficient energy transfer.

Twenty-three new materials were doped with the ion Eu^{+3}, and ratios of areas of the emission peaks $^1D_0 \rightarrow {}^7F_1$ (orange) to $^1D_0 \rightarrow {}^7F_2$ (red) were determined. The compounds $BaNaB_9O_{15}$ and $BaLiB_9O_{15}$ were found to exhibit the highest red to orange ratio among the tested materials.

The compound $SrLiB_9O_{15}$ has previously been examined as a possible nonlinear optical material. Following UV excitation, a bright green luminescence from a Ce, Tb codoped sample has been observed.

Unusual luminescence properties have recently been observed for the host $InBO_3$ and selected tellurites. In these materials, there appears to be sufficient overlap between the conduction band of the host and excited levels of selected dopants to give rise to a photooxidation of the dopant. To determine if this effect could be associated with an isolated In center, the compounds $Sr_3Sc(BO_3)_3$, $Sr_3In(BO_3)_3$, and $Sr_3Lu(BO_3)_3$, were doped with Bi^{+3}. Evidence for an ionization effect was not found, but a clustering of Bi^{+3} ions is proposed.

LUMINESCENT PROPERTIES OF INORGANIC OXIDES

by

Kimberly Hockaday Dahm

A THESIS

submitted to

Oregon State University

in partial fulfillment of
the requirements for the
degree of

Master of Science

Completed December 5, 1994
Commencement June 1995

Master of Science thesis of Kimberly Hockaday Dahm presented on December 5, 1994

APPROVED:

Redacted for Privacy

Major Professor, representing Chemistry

Redacted for Privacy

Chair of Department of Chemistry

Redacted for Privacy

Dean of Graduate School

I understand that my thesis will become part of the permanent collection of Oregon State University libraries. My signature below authorizes release of my thesis to any reader upon request.

Redacted for Privacy

Kimberly Hockaday Dahm

ACKNOWLEDGMENTS

I would like to thank my family for their support and faith in me during these last few years. My grandmother Ethel Crane-Hockaday has been an endless source of wisdom, patience, love and encouragement. My husband Matthew Dahm has given me the strength to continue and complete my studies.

My education would not have proceeded this far had it not been for Donny Granger. He instilled in me curiosity and a love of learning. His beliefs in education and the wonders of the universe have truly been inspirational to me.

The "old-timers" of my hometown must also be thanked for acting as my extended family. Their faith in me as well as their kind words has kept me going more than once. Their enthusiasm and warmth of spirit always let me know that my successes and trials were theirs as well.

I appreciate the help I received from my colleagues in the Keszler group as well as Dr. Keszler for all his assistance. I especially appreciate the help I was given from Dr. Annapoorna Akella and Junming Tu. I have learned a great deal from them both.

I would like to say a special thank you to Dr. Glenn Evans for his moral support and friendly advice. He has helped make graduate school a worthwhile endeavor.

TABLE OF CONTENTS

LIST OF FIGURES

LIST OF TABLES

Luminescent Properties of Inorganic Oxides

Chapter 1

Introduction

Phosphors are materials that absorb some form of energy and then emit part of this energy as light. This absorbed energy can be derived from IR, UV, or visible light, high energy electrons, a mechanical stress, or simple heat, to name just a few.[1] Phosphors have become an integral part of our everyday lives. They are used in fluorescent lamps, lasers, digital radiography, high definition television screens, fiber optics, and solar concentrators.[2,3,4] To meet the continuing demands and development of our technological society, the search for and development of phosphors having desirable characteristics continues.

Inorganic phosphor development is based largely on the interaction between a host and a selected dopant ion. The nature of this interaction, for example, determines for many ions both emission wavelengths and quantum efficiencies. In this work, I have selected to study this host-dopant interaction in several different materials by using the ions Bi^{+3}, Eu^{+2}, Ce^{+3}, Tb^{+3}, and Eu^{+3}. The luminescence characteristics of Bi^{+3} are highly dependent on the host lattice, producing a broad range of colors, widths, and Stokes shifts. It is commonly used to detect high energy radiation such as γ-rays.[5] The ion Eu^{+2} is currently finding a market in storage x-ray phosphors.[6] Like Bi^{+3}, it produces

host-dependent broad band emission and Stokes shifts. The ions Ce^{+3}, Tb^{+3}, Eu^{+3} (along with Eu^{+2}) have changed our fluorescent lighting forever.[7] The color rendition produced by compounds doped with these ions produces a visible spectrum that to our eye mimics well the solar spectrum.[8]

During the past several years, much effort in this lab has been directed to the synthesis of new materials that may serve as hosts for optically active ions. One such class of new compounds is the $A_6MM'(BO_3)_6$ family, designated STACK. In Chapter 2, I summarize some results on the luminescent properties of one member of this family, $Sr_6YAl(BO_3)_6$, that has been doped with a variety of luminescent ions. Another compound $SrLiB_9O_{15}$ was codoped with Ce^{+3} and Tb^{+3} to see if it might make a viable replacement for the currently used $(Ce,Gd)MgB_5O_{10}$: Tb^{+3}.[9] In Chapter 3, I describe results on red Eu^{+3} emission from 23 different hosts. This work represents the initial stages of an effort in this lab to identify new phosphors that may satisfy the rigorous requirements of new high definition displays and plasma display panels.[10] The compound $SrLiB_9O_{15}$ has been identified as a new host for the energy transfer process $Ce^{+3} \rightarrow Tb^{+3}$; results on this are given in Chapter 4. To probe the possible photoionization of oxidizable ions in the presence of an isolated In^{+3} ion, I have examined the luminescence characteristics of the ion Bi^{+3} in the isostructural hosts $Sr_3Sc(BO_3)_3$, $Sr_3Lu(BO_3)_3$, and $Sr_3In(BO_3)_3$. Results on these systems are summarized in Chapter 5.

All compounds were synthesized by using high-temperature solid state techniques and optically pure chemicals. Following characterization of each compound with powder X-ray diffraction techniques, luminescence spectra were obtained by a spectrometer (Figure 1.1) assembled by past members of the group. With a spectrum in hand, its features were analyzed on the basis of literature precedents, and specific characteristics of the host were identified.

Much of the information provided here should be useful for selecting materials that may prove to be useful phosphors. To further advance development of these materials, issues of efficiency, stability, processibility, thermal quenching, and luminescence lifetimes must be addressed.

Eu^{+3} Fluorescence Characteristics

Compounds doped with Eu^{+3} ions consist of $^5D_0 \rightarrow {}^7F_j$ emissions (see Figure 1.2)[11]. This process involves f→f type transitions in which not only electric dipole transitions but also magnetic dipole transitions, are prohibited. Electric dipole transitions are forbidden by the Laporte selection rules because there is no change in parity between the ^5D and ^7F states. They are magnetic dipole forbidden because the total angular momentum changes from 2 to 3.[12]

Luminescence from the Eu^{+3} ion is possible because both rules can be relaxed. The spin prohibition is relaxed through spin orbit coupling. The ^7F states can be described as a mixture of pure ^7F states plus pure ^5D states. As a result of this mixing of states, the rule is not as strict. The parity restriction can

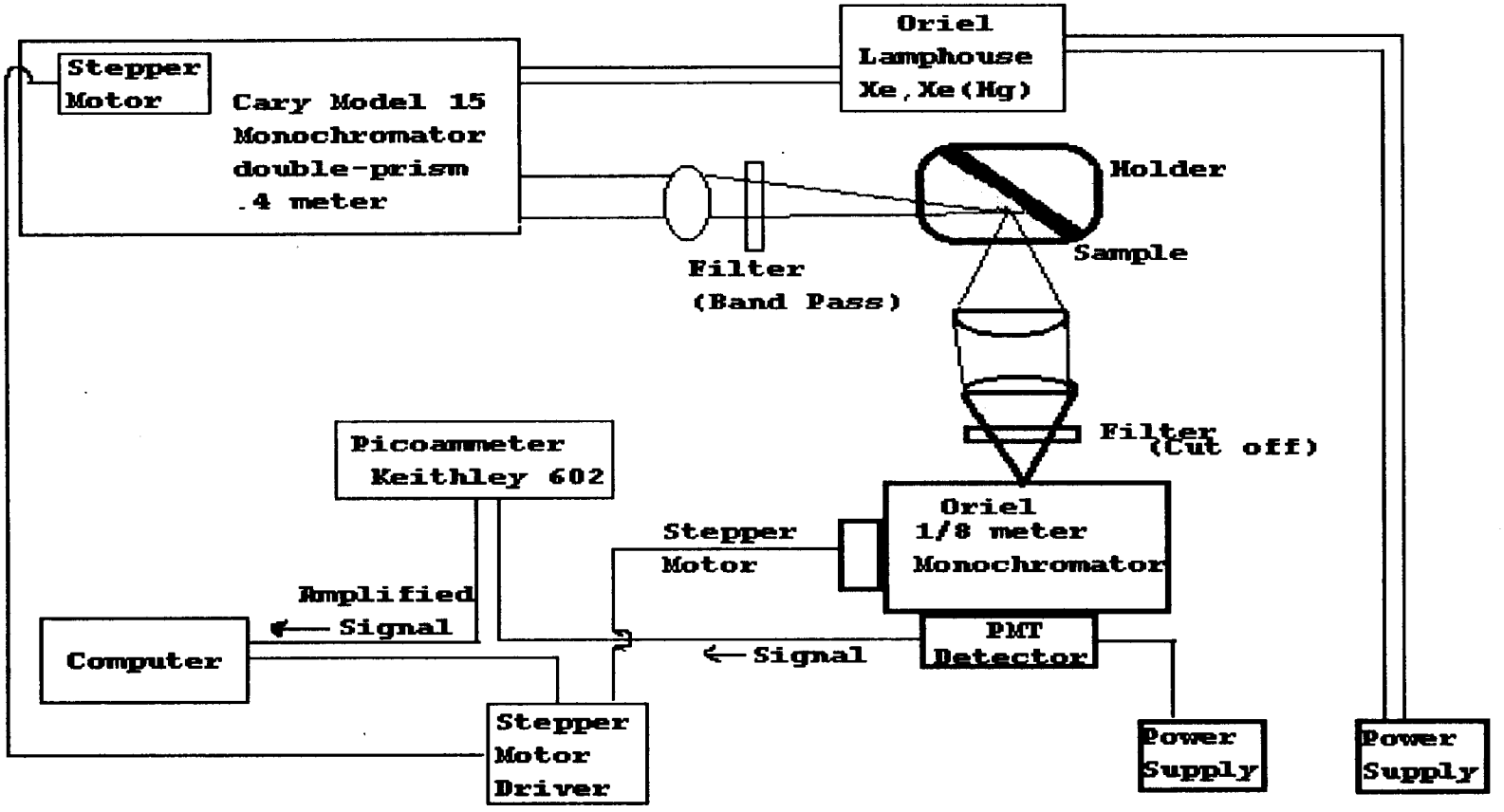

Figure 1.1 Diagram of Keszler Lab Spectrometer

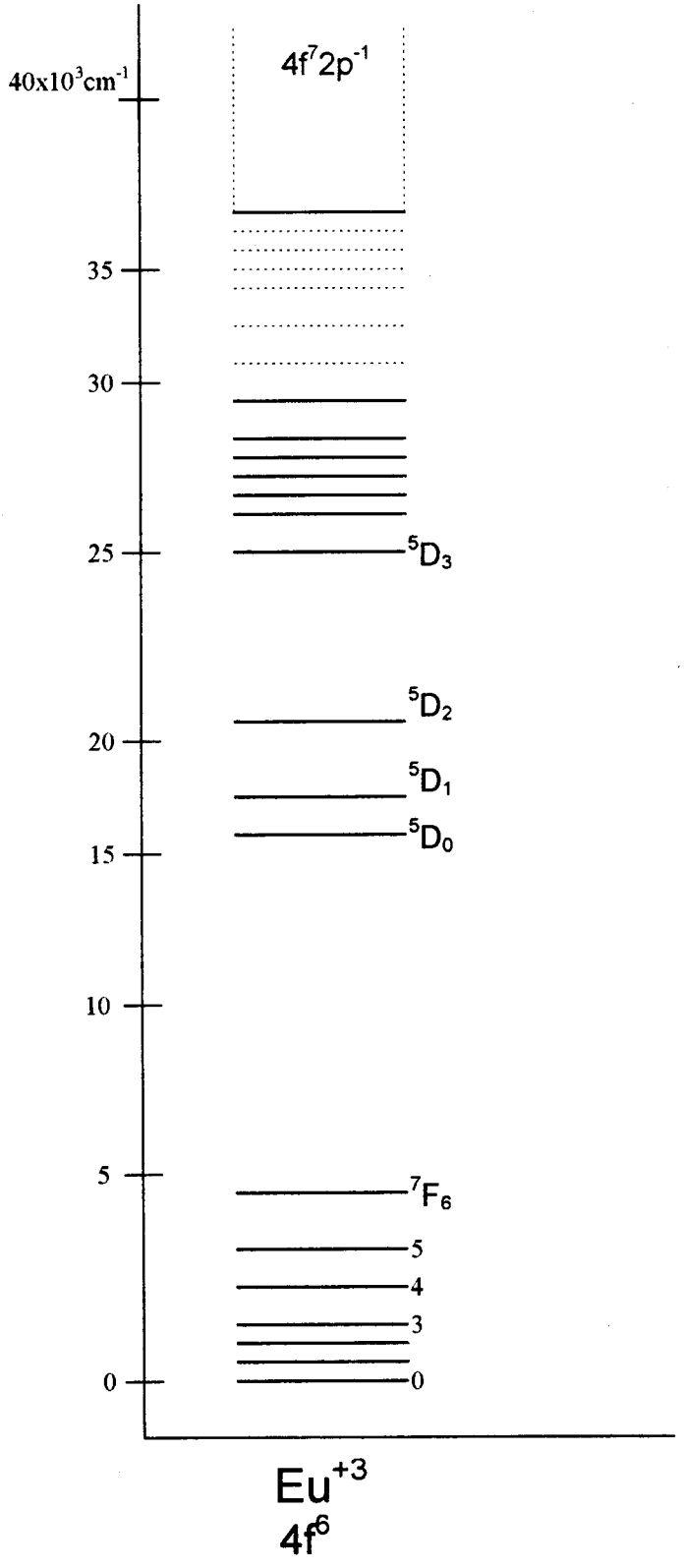

Figure 1.2 Energy Level Diagram for Eu^{+3} ion

only be relaxed through the influence of the crystal lattice. The $4f^6$ state of the Eu^{+3} ion must be mixed with a state of different parity to make it less Laporte forbidden. The forced electric dipole transitions are brought about by the addition of odd crystal field terms.

Since the parity restriction only relaxes with the addition of odd crystal field terms, the lattice must not contain a center of inversion. A lattice possessing a center of symmetry cannot contribute odd crystal field terms and as a result the parity prohibition remains. Magnetic dipole transitions will take place because of spin orbit coupling. Therefore a lattice that is centrosymmetric will have only one allowed transition: $^5D_0 \rightarrow {}^7F_1$ thereby producing an orange emission.[13]

A noncentrosymmetric lattice allows the addition of the odd crystal field terms. This allows both magnetic dipole as well as the forced electric dipole transitions to be present. The spectrum will now show transitions of $^5D_0 \rightarrow {}^7F_1$ (orange) from the magnetic dipole, and well as $^5D_0 \rightarrow {}^7F_{2,4,6}$ (red) from the electric dipole.[14] Electric dipole transitions are stronger than magnetic, so the $^5D_0 \rightarrow {}^7F_2$ is expected to be the most intense peak, producing a red luminescence in the compound.

References

1. G. R. Fonda and E. F. Apple, *Luminescent Materials*, Encyclopedia of Chemical Technology, **14**, 527, (1981).

2. L.J. Andrews, G.H. Beall and A. Lempicki, *J. Luminescence* **36**, 65, (1986).

3. K. Takahashi, J. Miyahara and Y. Shibajara, *J. Electrochem. Soc.* **132**, 1492, (1985).

4. G. Blasse, *Mat. Chem. Phys.* **16**, 201, (1987).

5. G. Blasse, *Chem. Mat.* **1**, 298, (1989).

6. M. K. Crawford and L.H. Brixner, *J. Luminescence* **48 & 49**, 37, (1991).

7. B.M.J. Smets, *Mat. Chem. Phys.* **16**, 284, (1987).

8. T. Welker, *J. Luminescence* **48 & 49**, 49, (1991).

9. Welker, 53.

10. H. Yamamoto and H. Matsukiyo, *J. Luminescence* **48 & 49**, 44, (1991).

11. Michael D. Lumb,ed., Luminescence Spectroscopy, Academic Press, NY, 21, (1978).

12. Paul Goldberg, ed., Luminescence of Inorganic Solids, Academic Press, NY, 21, (1966).

13. H.M. Crosswhite and H.W. Moos, ed., Optical Properties of Ions In Crystals Interscience Publishers, NY 162, (1967).

14. G. Blasse and A. Bril, *Philips Technical Review* **31**, 310, (1970).

Chapter 2

Luminescent Characterization of Doped $Sr_6YAl(BO_3)_6$

Abstract

$Sr_6YAl(BO_3)_6$ was doped with a series of optically active ions to determine its optical properties. The ions used were Bi^{+3}, Pb^{+2}, Ce^{+3}, Eu^{+2}, Eu^{+3}, and Tb^{+3}. The spectra were recorded and analyzed for unique features that may make this compound commercially viable.

Introduction

The compound $Sr_6YAl(BO_3)_6$ is a member of a recently discovered class of compounds that has been designated STACK. STACK consists of the general formula of $A_6MM'(BO_3)_6$, where A = Sr, Ba, Pb, or a selected lanthanide; M = Ca, Sr Y, Sc, In, Bi, or a selected lanthanide; and M' = Mg, Al, Cr, Mn, Fe, Co, Rh, Zn, Sc, In, Zr, Hf, Sn, or a selected lanthanide. The structure is comprised of chains of distorted octahedra that are occupied by atoms M or M' and separated by triangular planar BO_3 groups. The A atom is bound by O atoms in a 9-coordinate site, and the M and M' atoms are also bound by O atoms in 6-coordinated, distorted octahedral sites.[1]

The purpose of this investigation was to study the luminescence properties of $Sr_6YAl(BO_3)_6$ doped with selected ions. One other member of the

STACK family, $Sr_3Sc(BO_3)_3$ has been proposed as a potential new laser material when doped with Cr^{+3}.[2] Because the essential structural features of the STACK family vary little with various substitutions at the A, M, and M' sites, it is expected that the many STACK compounds will have similar spectra for some luminescent dopants. The transparent derivative $Sr_6YAl(BO_3)_6$ should then provide characteristics that are representative of this family of compounds.

Experimental

Powder samples of $Sr_6YAl(BO_3)_6$, were prepared by standard high-temperature solid-state methods. Stoichiometric quantities of $Sr(NO_3)_2$, Y_2O_3, and Al_2O_3, (all typically ≥ 99.9% purity) were mixed with a 3 mol % excess of B_2O_3 and 1 mol % of a selected dopant-- Bi_2O_3, Ce_2O_3, Eu_2O_3, PbO, $Tb(NO_3)_3 \bullet 5H_2O$, and KNO_3 (to charge balance when necessary). The samples were ground under hexane and heated in a platinum crucible at 923 K for 30 min followed by regrinding and heating to 1340 for 12 h. The samples of Ce^{+3} and Eu^{+2} were heated to 1340 K under a H_2/N_2 reducing atmosphere for 24 hours. The resulting powders were confirmed to be single phase by comparing their diffraction patterns to the known pattern of $Sr_6YAl(BO_3)_6$.

Spectral data was obtained by using a spectrometer assembled in this laboratory, specifically designed for solid samples. (See Figure 1.1). The powder sample was mounted on a cardboard holder and held in place by a non-optically active grease. For excitation spectra, the appropriate wavelength of

light was selected with a Cary model 15 prism monochromator from an Oriel 300 W Xe lamp. The emission wavelengths for all spectra were scanned by using an Oriel model 22500 1/8-m monochromator. Appropriate filters were positioned to block undesirable wavelengths of light. The signal was detected with a Hamamatsu R636 photomultiplier tube and amplified with a Keithley model 602 picoammeter. The signal was then digitized for computer acquisition and analysis. Spectrometer control software was written in this laboratory.

Results and Discussion

$Sr_6YAl(BO_3)_6$ crystallizes in the space group R3. Y and Sr were determined to be the doping sites based on luminescence data. Y has an octahedral coordination, surrounded by 6 oxygen versus the Sr site which is coordinated by 9 oxygen atoms (Figure 2.1).

The doped sample Bi^{+3}: $Sr_6YAl(BO_3)_6$ produces a broad band emission with a maximum emission of 424 nm (Figure 2.2) and an excitation maximum at 314 nm. Because Bi^{+3} is characterized by a $6s^2$ ground state configuration and a $6s^16p^1$ excited-state configuration, its luminescence is very host dependent. This host dependency can be seen in the Stokes shift of 8.2×10^3 cm^{-1}. This is a smaller shift than those observed in Bi_2GeO_{20} (20.2×10^3 cm^{-1}) and $Bi_2Al_4O_9$ (17.7×10^3 cm^{-1}),[3] comparable to that observed in YBO_3 (8.2×10^3 cm^{-1}), and larger than that of $YAl_3B_4O_{12}$ (2×10^3 cm^{-1})[4] and $ScBO_3$ (2×10^3 cm^{-1})[5]. It is known from single-crystal X-ray studies that the ion La^{+3} occupies the A site.

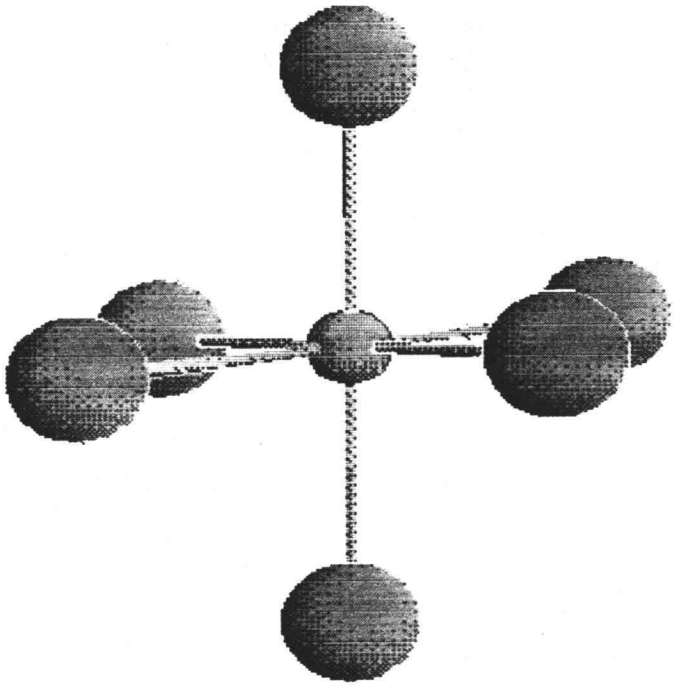

Y surrounded by 6 oxygen atoms

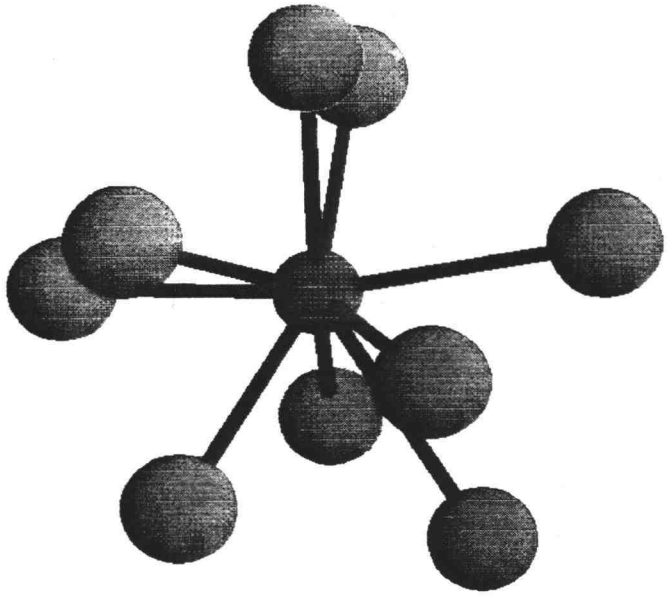

Sr surrounded by 9 oxygen atoms

Figure 2.1 Coordination of Y and Sr atoms in $Sr_6YAl(BO_3)_6$

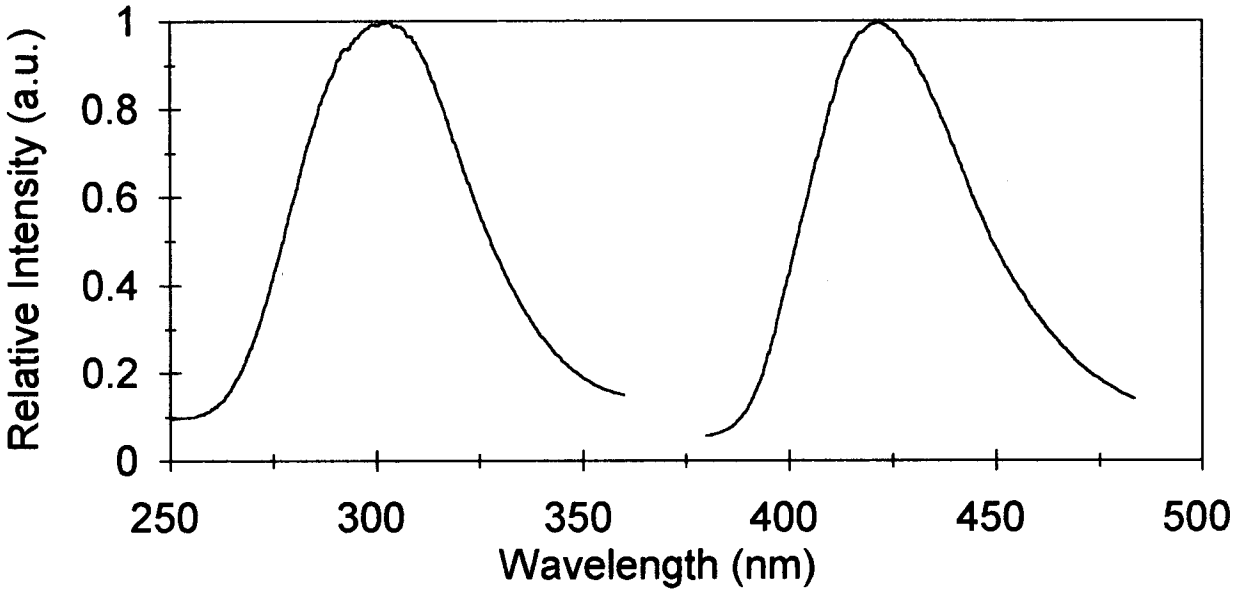

$\lambda_{exc.\ max}$= 314 nm

$\lambda_{em.\ max}$= 424 nm

Figure 2.2 Luminescence Spectra of 1% Bi^{+3}: $Sr_6YAl(BO_3)_6$

Because the Bi^{+3} ion has a crystal radius that is equivalent to La^{+3}, it is also expected to occupy the A site. The magnitude of the Stokes shift appears to be consistent with this assertion. The relatively low-energy position of the excitation band is also inconsistent with placement of the Bi^{+3} ion on an octahedral site.

This was also the situation in the Pb: $Sr_6YAl(BO_3)_6$, which emitted in the violet with a maximum of 406 nm (Figure 2.3). The excitation maximum is at 277 nm. The emission is from the allowed transition of $^3P_1 \rightarrow {}^1S_0$ which, like Bi^{+3}, derives from $6s^16p^1$ excited and $6s^2$ ground states respectively. The Stokes shift was 11.5 x 10^3 cm^{-1}, similar compared to compounds like $PbGe_3O_9$ (12.9 x 10^3 cm^{-1}) and $PbAl_2O_4$ (19.4 x 10^3 cm^{-1}).[6] The Stokes shift is like Bi^{+3} indicative of Pb^{+2} occupying the Sr^{+2} site.

The characteristics of Ce^{+3} : $Sr_6YAl(BO_3)_6$ are similar to those of Bi^{+3}, The large Stokes shift of 8.3 x 10^3 cm^{-1} (Figure 2.4) may be compared with those of the compounds $ScBO_3$: Ce (1.2 x 10^3 cm^{-1}), YBO_3: Ce (2.0 x 10^3 cm^{-1}) and $Y_3Al_5O_{12}$: Ce (3.8 x 10^3 cm^{-1}).[7] The maximum emission due to the 5d→4f transition, occurs at 412 nm. The maximum absorption was found at 307 nm. The absorption band from 250 to 350 nm appeared as several peaks overlapping and may refine at lower temperatures. If so, this would indicate some crystal field splitting of the $5d^1$ excited state.[8] The large Stokes shift suggested that Ce, like Bi^{+3} resided on the Sr site. This can be compared with

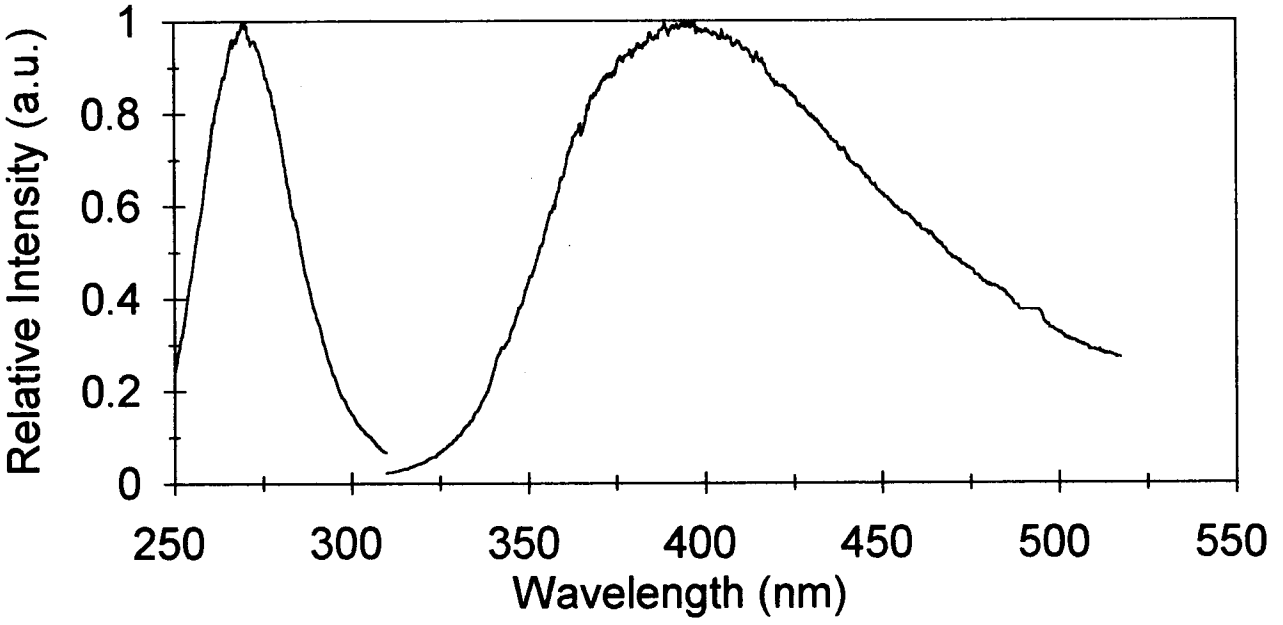

$\lambda_{exc.\ max}$= 277 nm

$\lambda_{em.\ max}$= 406 nm

Figure 2.3 Luminescence Spectra of 1% Pb^{+2}: $Sr_6YAl(BO_3)_6$

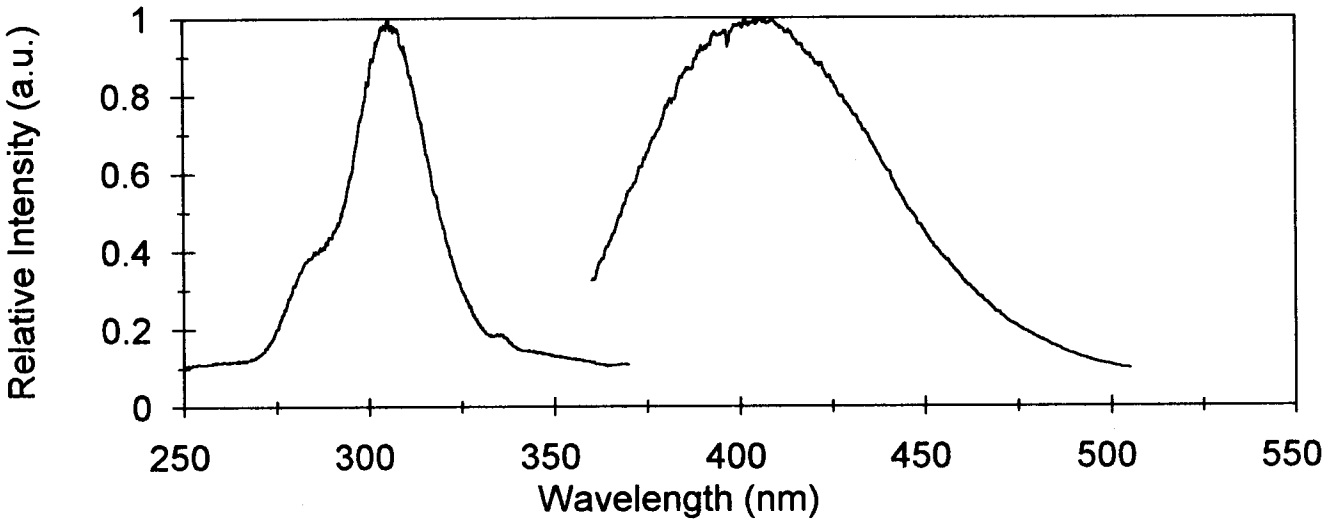

$\lambda_{exc.\ max}$= 307 nm

$\lambda_{em.\ max}$= 412 nm

Figure 2.4 Luminescence Spectra of 1% Ce^{+3}: $Sr_6YAl(BO_3)_6$

$ScBO_3$ and YBO_3 where the Ce^{+3} ion resides in octahedral sites[10] and small Stokes shifts are observed.

Eu^{+2}: $SrYAl(BO_3)_6$ was prepared by using a precursor of $Sr_3B_2O_6$: 2% Eu^{+2}. This was then mixed with the other components and placed into a reducing atmosphere for four days. Direct reduction of Eu_2O_3 in $SrNO_3$, Al_2O_3, and Y_2O_3 is not possible even with a prolonged reducing environment. Like its precursor, Eu^{+2} had a yellow luminescence[10]. The maximum absorption was found at 311 nm. The maximum emission, arising from the $4f^65d \rightarrow {}^8S_{7/2}$ transition, was found at 587 nm, producing a Stokes shift of 15.1 x 10^3 cm^{-1} (Figure 2.5). The two peaks in the excitation region produced two possibilities: unreduced Eu^{+3} or crystal field splitting. Given the small Stokes shift of the preceding compounds, it is more likely that the Eu^{+2} ion was doped onto the Sr^{+2} site, which would give rise to crystal field splitting. The large Stokes shift and the consequent low-lying excitation band suggest a low quenching temperature should be found[11].

Tb^{+3}: $SrYAl(BO_3)_6$ produces a spectrum with a maximum emission from the ${}^5D_4 \rightarrow {}^7F_5$ transition at 552 nm (Figure 2.6) . The excitation had a maximum at 265 nm. The four bands of the emission have been assigned to the four transitions of ${}^5D_4 \rightarrow {}^7F_{6,5,4,3}$ respectively. The excitation had transitions from the charge transfer band ($4f^75d$), ${}^7F_6 \rightarrow {}^7D_2$, ${}^7F_6 \rightarrow {}^5L_{10}$, ${}^7F_6 \rightarrow {}^7D_3$. The unfavorable overlap of the excitation maximum with the Ce^{+3}: $SrYAl(BO_3)_6$ emission maximum make this compound an unfavorable candidate for $Ce^{+3} \rightarrow Tb^{+3}$.

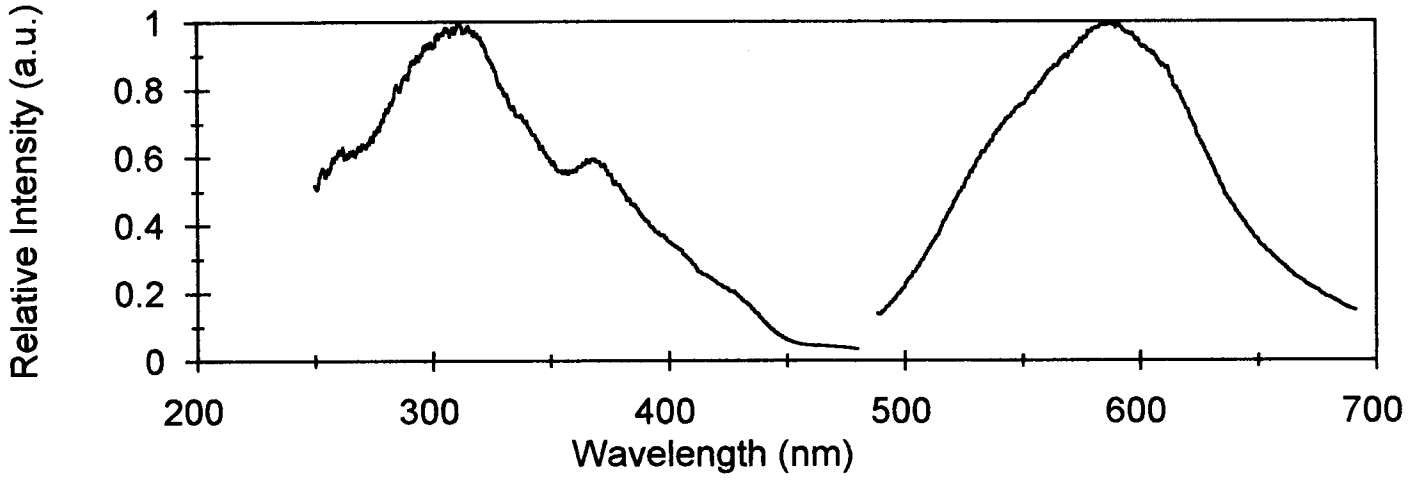

$\lambda_{exc.\ max}$= 311 nm

$\lambda_{em.\ max}$= 587 nm

Figure 2.5 Luminescence Spectra of 1% Eu^{+2}: $Sr_6YAl(BO_3)_6$

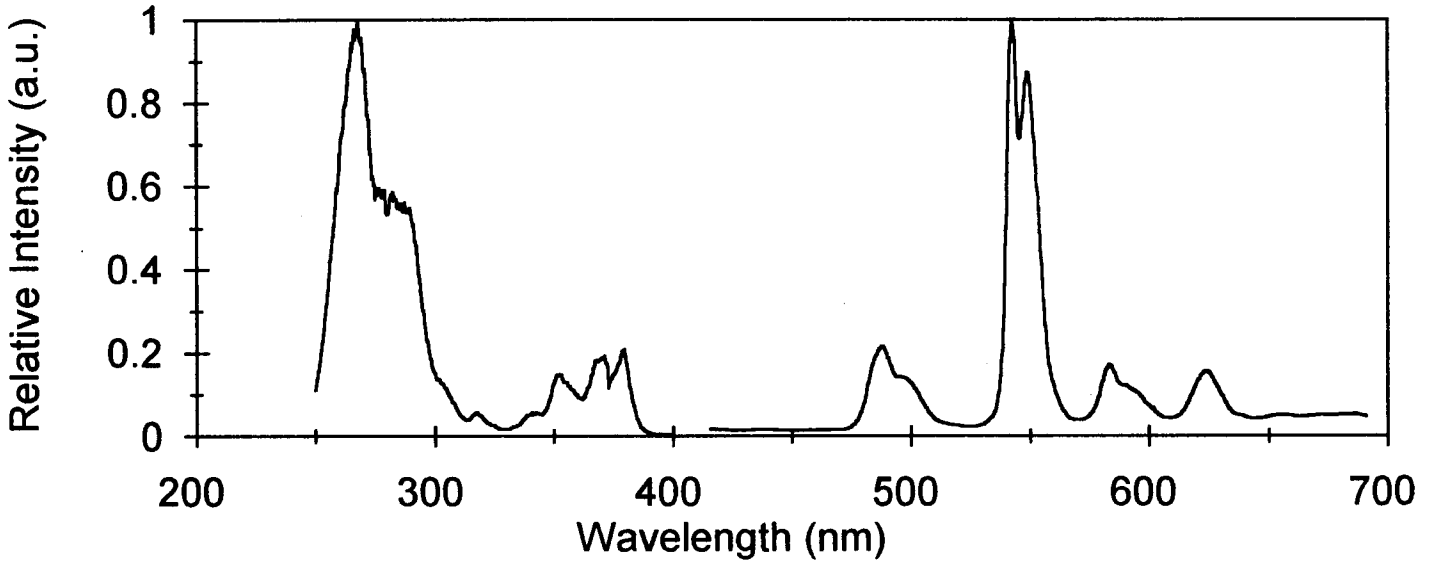

$\lambda_{exc.\ max}$= 265 nm

$\lambda_{em.\ max}$= 552 nm

Figure 2.6 Luminescence Spectra of 1% Tb^{+3}: $Sr_6YAl(BO_3)_6$

Eu^{+3}: $SrYAl(BO_3)_6$ produces an orange-red luminescence with a maximum emission at 612 nm (Figure 2.7). The maximum excitation was found to be located at 300 nm. The emission peaks are from $^5D_0 \rightarrow {}^7F_{0\text{-}4}$ transitions. The ratio of the red to orange peaks of $^5D_0 \rightarrow {}^7F_2/{}^5D_0 \rightarrow {}^7F_1$ is 1:1.23, (See Chapter 3). This ratio and the doubling of the emission peaks is consistent with a substitution of the Eu^{+3} ion on both the Y^{+3} and Al^{+3} sites.

Further testing of quantum efficiencies and thermal quenching are on-going to more fully characterize the optical properties of these materials.

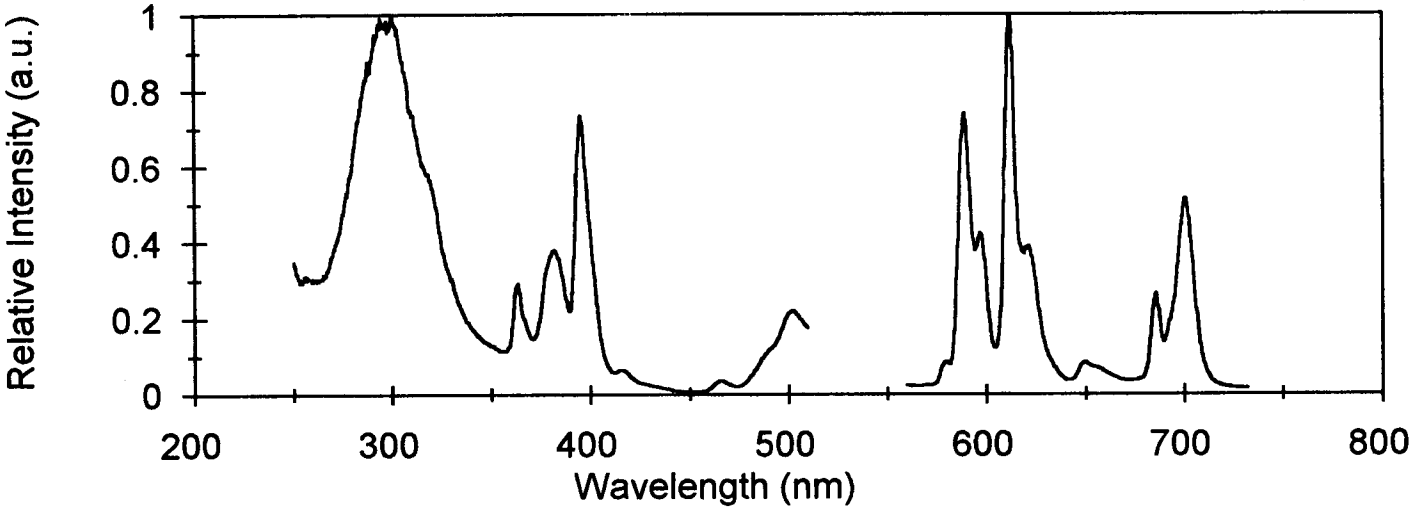

$\lambda_{exc.\ max}$= 300 nm

$\lambda_{em.\ max}$= 612 nm

Figure 2.7 Luminescence Spectra of 1% Eu^{+3}: $Sr_6YAl(BO_3)_6$

References

1. K.I. Schaffers, P.D. Thompson, T. Alekel, J.R. Cox, and D.A. Keszler, Chem. Mater., in press.

2. P.D. Thompson and D.A. Keszler, Chem. Mater. 1, 292, (1989).

3. C.W.M. Timmermans, and G. Blasse, *Solid State Chem* **52**, 228 (1984).

4. G. Blasse and A. Bril, *J Chem Phys* **47**, #6, 1921 (1967).

5. G. Blasse and C. de Mello Denega, *Solid State Comm* **91**, 30 (1994).

6. Timmermans, ibid, 228.

7. G. Blasse and A. Bril, *Progress Solid State Chem.* **18**, 79 (1988).

8. G. Blasse and A. Bril, *J Chem Phys* **47**, 5140 (1967).

9. G. Blasse and A. Bril, *J Chem Phys* **47**, 5140 (1967).

10. A. Wolfert, E. Oomen and G. Blasse, *J Luminescence* **31**, 308 (1984).

11. B. DiBartolo, ed., Radiationless Processes, Plenum Press, NY, 287 (1980).

12. W.J. Schipper, D. van der Voort, P. van den Berg, Z.A.E.P. Vroon and G. Blasse, *Mater Chem Physics*, **33**, 312 (1993).

Chapter 3

Red Luminescence of Eu^{+3} in Selected Hosts

Abstract

Twenty three compounds were doped with 1% Eu^{+3} to determine the integrated red to orange ratios in the luminescence bands. These were compared to the industry standard of Y_2O_3. Of the compounds tested, $BaNaB_9O_{15}$ and isostructural $BaLiB_9O_{15}$ possessed the highest ratio, while $Sr_6YSc(BO_3)_6$ and $Sr_6YAl(BO_3)_6$ possessed the lowest.

Introduction

The nature of the red phosphor in fluorescent lamps and color television screens is paramount to producing a high quality color rendition.[1] Thus far the industry standard is Y_2O_3: Eu^{+3}, which is used primarily in low pressure fluorescent lamps and color TV screens.[2] Its high efficiency and narrow bandwidth make it an exceptional red phosphor but its high cost makes it desirable to pursue other alternatives.[3]

When looking for alternatives, it is important to identify materials having non-centrosymmetric dopant sites. This allows for a large integrated ratio of the $D_0 \rightarrow {}^7F_2$ (red) to $D_0 \rightarrow {}^7F_1$ (orange) peaks, leading to a deeper red phosphor. The

charge transfer band must also occur at high energy to insure high quantum efficiency and quenching temperatures.[4]

Recent advances in the development of plasma display panels provide an additional impetus to examine new materials. These flat panels operate by photoexcitation of a phosphor near 150 nm through a rare-gas discharge. In this application, the phosphor must absorb the 150 nm excitation and exhibit stability to this high-energy radiation as well as the ions in the plasma. Borates have absorption edges in the range 160-190 nm, so they can absorb the high-energy light, and exceptional optical damage thresholds have been demonstrated. At the present time, the mixed orthoborate Eu^{+3}: $Y_{0.5}Gd_{0.5}BO_3$ is, in fact, used in this application.

Experimental

Powder samples of all compounds were prepared by standard high temperature solid-state methods. Stoichiometric quantities of reagent grade oxides, nitrates, and carbonates ($\geq$ 99.9% purity) were mixed with B_2O_3, 1% Eu_2O_3, and KNO_3 (to charge balance when necessary) and ground under hexane. The nitrates and carbonates were decomposed in a platinum crucibles at 923 K for 30 min followed by regrinding and heating to appropriate temperatures for up to 48 h. The resulting powders were confirmed to be single phase and the correct structure by comparing their diffraction patterns to calculated patterns.

Spectral data was obtained by using the methods outlined in previous chapters and software written in this laboratory. Peak areas were measured using Quattro Pro™ (windows version) and Peakfit™ (Jandel Software). Quattro Pro™ was initially used to locate and graph the relevant transitions. The data was then imported into Peakfit™ where each transition was fitted with Gaussian peaks. A curve fitting process was run to integrate the area under each curve. This integrated area was then used as a guide to calculate the ratio of integrated areas beneath the transitions.

Results and Discussion

Results for the 23 compounds examined in this study are summarized in Tables 3.1 and 3.2. The industrially important hosts Y_2O_3 and $Y_{.5}Gd_{.5}BO_3$ are included in these listings. The red-to-orange ratio varies from a low of 1.23:1 for the host $Sr_6YAl(BO_3)_6$ to a high of 4.78:1 for the host Y_2O_3. Several compounds, including $BaCaBO_3F$, $Ba_2LiB_5O_{10}$, $Sr_2Mg(BO_3)_2$, and the family $MM'B_9O_{15}$ (M=Sr, Ba, M'= Li, Na), exhibit ratios greater than 3:1.

The compound Y_2O_3 contains two crystallographically distinct Y^{+3} sites, each bound by six O atoms. One site has S_6 symmetry and is easily described as a distorted octahedron. The other site, having C_2 symmetry, is best described as a distorted placement of O atoms at six of the eight corners of a cube.[5] Efficient energy transfer from the S_6 site ($^7D_0 \rightarrow {}^7F_{0,1}$) to the C_2 site ($^7D_0 \rightarrow {}^7F_2$) produces an intense peak at 612 nm.[6] The Eu^{+3} ion, having a larger

COMPOUND	CT Position[a] (nm)	RATIO[b] (Orange to Red)	r^{2c}
Y_2O_3	350	1:4.8	0.975
$BaNaB_9O_{15}$	315	1:3.9	0.999
$BaLiB_9O_{15}$	315	1:3. 9	0.999
$Ba_2LiB_5O_{10}$	354	1:3.3	0.999
$BaCaBO_3F$	N/A	1:3.3	0.996
$Sr_2Mg(BO_3)_2$	357	1:3.2	0.999
$SrLiB_9O_{15}$	356	1:3.1	0.999
$CaLiBO_3$	313	1:2.8	0.999
$Ba_3Y(BO_3)_3$	N/A	1:2.6	0.98
$BaLiBO_3$	350	1:2.6	0.999
$BaNaB_5O_9$	352	1:2.6	0.999
$Y_{.5}Gd_{.5}BO_3$	N/A	1:2.6	0.998
$Ba_2Mg(BO_3)_2$	N/A	1:2.5	0.994
$SrKB_5O_9$	354	1:2.4	0.999
$CaNaB_5O_9$	354	1:2.3	0.999
$GdBO_3$	N/A	1:2.2	0.998
YBO_3	N/A	1:2.2	0.997
$Sr_4Ge_2O_7F_2$	355	1:2.1	0.999
$SrLiBO_3$	353	1:2.0	0.999
Sr_2LiSiO_4F	350	1:2.0	0.999
$Ba_2Ca(BO_3)_2$	355	1:1.9	0.998
$Sr_6ScY(BO_3)_6$	350	1:1.6	0.994
$Sr_6YAl(BO_3)_6$	355	1:1.2	0.999

[a]onset wavelength for charge-transfer transition

[b]ratio of integrated intensities for $^7D_0 \rightarrow {}^7F_1$ / $^7D_0 \rightarrow {}^7F_2$

[c]error associated with the peak fit of the proposed curve to the actual curve.

Table 3.1 Red to Orange Ratios of Eu^{+3} in Selected Oxide Hosts.

COMPOUND	Excitation Maximum[a] (nm)	Emission Maximum (nm)	Ratio of heights of $F_0 \rightarrow D_2$ / $F_0 \rightarrow D_1$
Y_2O_3	250*	613	7.8
$BaNaB_9O_{15}$	256*	615	4.1
$BaLiB_9O_{15}$	261*	615	4.5
$Ba_2LiB_5O_{10}$	273*	615	3.0
$BaCaBO_3F$	390	611	4.0
$Sr_2Mg(BO_3)_2$	395	616	2.2
$SrLiB_9O_{15}$	268*	617	3.2
$CaLiBO_3$	395	614	1.6
$Ba_3Y(BO_3)_3$	N/A	619	1.8
$BaLiBO_3$	394	617	1.7
$BaNaB_5O_9$	394	617	1.9
$Y_{.5}Gd_{.5}BO_3$	394	629	1.1
$Ba_2Mg(BO_3)_2$	395	619	1.5
$SrKB_5O_9$	394	620	1.5
$CaNaB_5O_9$	286	617	2.8
$GdBO_3$	274	629	1.0
YBO_3	395	614	0.9
$Sr_4Ge_2O_7F_2$	395	618	2.0
$SrLiBO_3$	394	616	1.8
Sr_2LiSO_4F	291	614	1.6
$Ba_2Ca(BO_3)_2$	395	615	1.3
$Sr_6ScY(BO_3)_6$	293	614	1.5
$Sr_6YAl(BO_3)_6$	300	612	1.4

[a]Charge-transfer excitation are indicated by *

Table 3.2 Excitation and Emission Maxima for Eu^{+3} in Selected Oxide Hosts.

radius than Y^{+3}, forces an even greater distortion of the noncentrosymmetric site. All of these factors, combined with a high energy charge transfer band (maximum at 244 nm), make for an efficient red phosphor.

Other than Y_2O_3, the highest red-to-orange ratios were observed for the two compounds $BaNaB_9O_{15}$ and $BaLiB_9O_{15}$. As seen in Figure 3.1, $BaNaB_9O_{15}$ has a 9-coordinate Ba site, and $BaLiB_9O_{15}$ has a 12-coordinate Ba site, each having C_3 symmetry.[7] Both lack a center of symmetry; only small displacements in the Ba and O positions result in the different coordination environments. As a result, excitation and emission characteristics are similar. Except for shorter Sr-O distances, the Sr environment in $SrLiB_9O_{15}$ is similar to the Ba sites of the corresponding Ba analogues. The red-to-orange ratio is smaller, however, and the charge transfer band is also positioned at a lower energy.

The smaller values of the red-to-orange ratios are largely associated with the centrosymmetric character of the dopant sites. For instance, the octahedral Ca site (symmetry C_{2h}) of $Ba_2Ca(BO_3)_2$ contains no center of symmetry, but the maximum deviation from orthogonal O-Ca-O angles is only 8°.[9] In the compounds $Sr_6YSc(BO_3)_6$, and $Sr_6YAl(BO_3)_6$ the Y site does possess a center of symmetry, but each compound still exhibits a greater red than orange emission, indicating a noncentrosymmetric site. In the development of the crystal chemistry of the STACK family of compounds[10], Schaffers, Alekel, Cox, et. al. found that the smaller, heavier lanthanides prefer occupation of the M(Y) site, whereas the larger, lighter lanthanides prefer occupation of the Sr site. Since

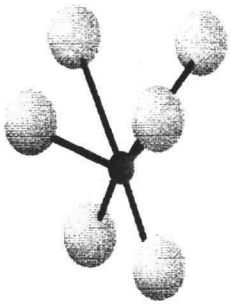

Y_2O_3: Y surrounded by 6 O
--C_2 site

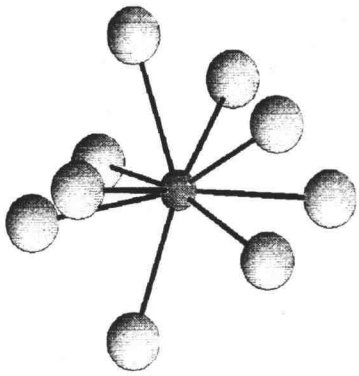

$BaNaB_9O_{15}$: Ba surrounded by
9 O atoms--C_3 site

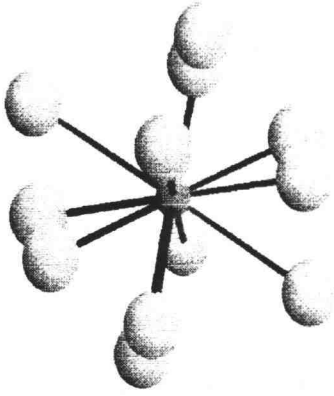

$BaLiB_9O_{15}$: Ba surrounded by 12 O
--C_3 site

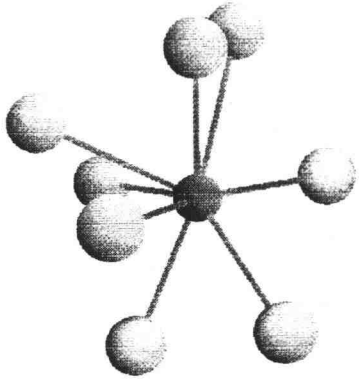

$Ba_2LiB_5O_{10}$: Ba surrounded by
8 O atoms--C_1 site

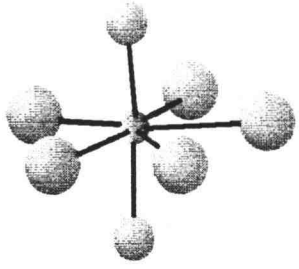

$BaCaBO_3F$: Ca surrounded by 5 O
and 2 F atoms--C_{2h} site

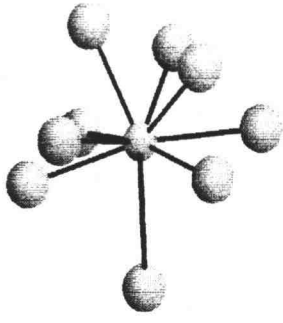

$Sr_2Mg(BO_3)_2$: Sr surrounded by
9 O atoms--C_1 site

Figure 3.1 Site Symmetry of Eu^{+3} Doped Compounds

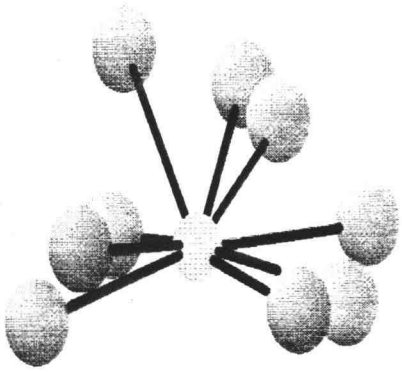

$SrLiB_9O_{15}$: Sr surrounded by 9 O
--C_3 site

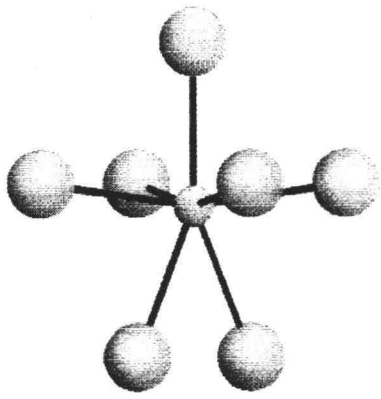

$CaLiBO_3$: Ca surrounded by 7 O
--C_2 site

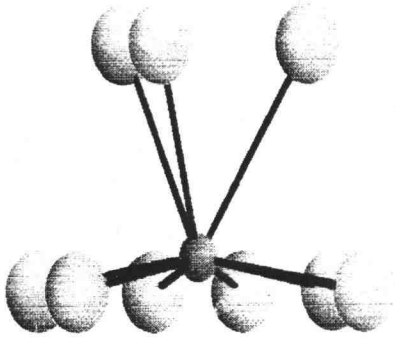

$Ba_3Y(BO_3)_3$: Ba surrounded by 9 O
--C site

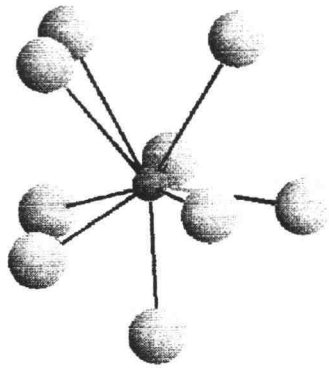

$BaLiBO_3$: Ba surrounded by 9 O
--C_1 site

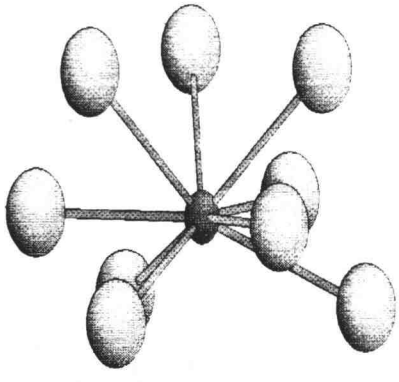

$BaNaB_5O_9$: Ba surrounded by 9 O
--C_1 site

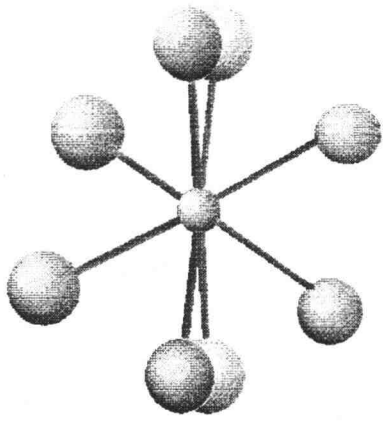

$Y_{.5}Gd_{.5}BO_3$: --C_{1v} site

Figure 3.1 continued Site Symmetry of Eu^{+3} Doped Compounds

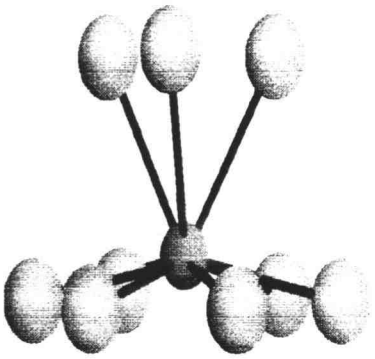

$Ba_2Mg(BO_3)_2$: Ba surrounded by 9 O
--D_{3d} site

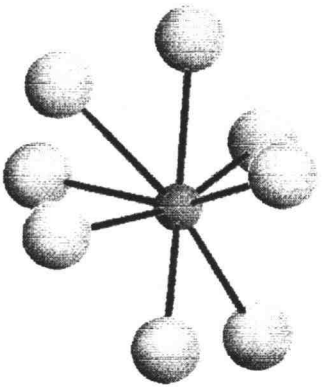

$SrKB_5O_9$: Sr surrounded by 8 O
--C_1 site

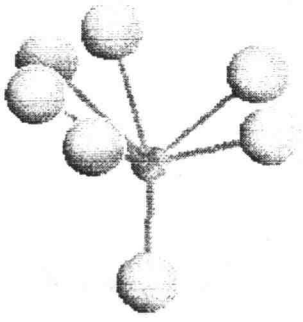

$CaNaB_5O_9$:[8] Ca surrounded by 7 O
--C_1 site

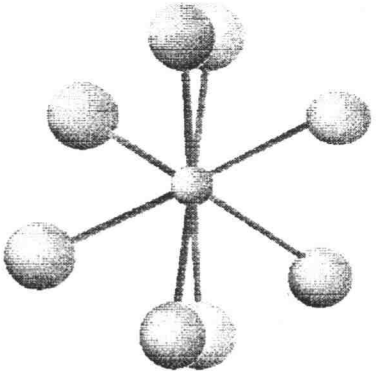

$GdBO_3$: Gd surrounded by 8 O
--C_{1v} site

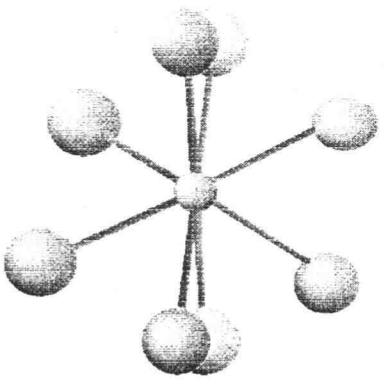

YBO_3: Y surrounded by 8 O
--C_{1v} site

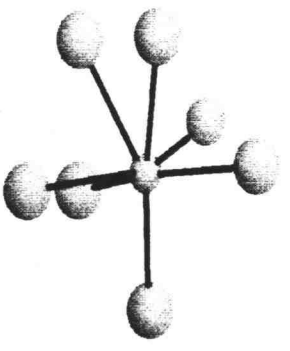

$Sr_4Ge_2O_7F_2$: Sr surrounded by 6 O
and 1 F atom--C_1 site

Figure 3.1 continued Site Symmetry of Eu^{+3} Doped Compounds

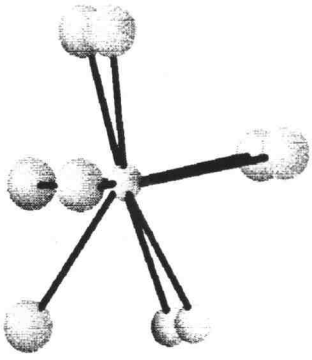

Sr_2LiSiO_4F: Sr surrounded by 7 O and 2 F atoms--C_s site

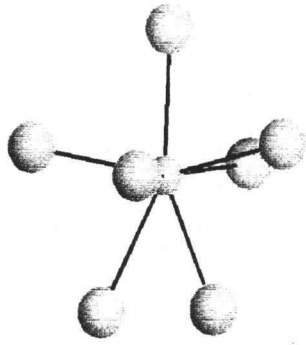

$SrLiBO_3$: Sr surrounded by 7 O --C_1 site

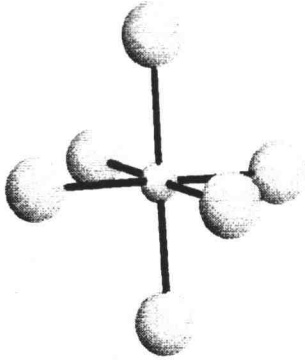

$Ba_2Ca(BO_3)_2$: Ca surrounded by 6 O --C_{2h} site

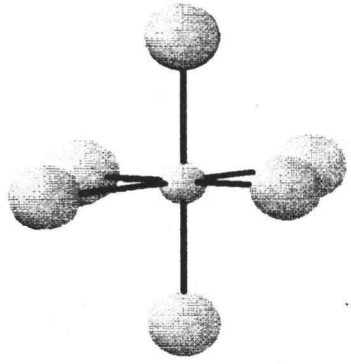

$Sr_6ScY(BO_3)_2$: Sc surrounded by 6 O ----S_6 site

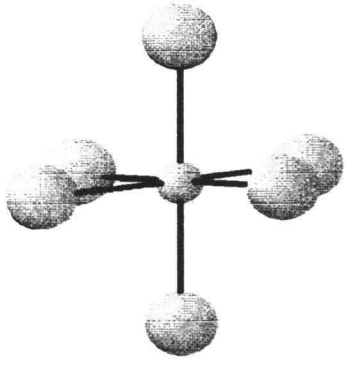

$Sr_6YAl(BO_3)_2$: Y surrounded by 6 O ----S_6 site

Figure 3.1 continued Site Symmetry of Eu^{+3} Doped Compounds

Eu^{+3} is intermediate in size, a mixed occupation of the Sr and Y sites should be anticipated. The relatively large red-to-orange ratio for these materials may arise from a distribution of the Eu^{+3} ions over both the centrosymmetric Y^{+3} sites and the noncentrosymmetric Sr^{+2} sites.

The positions of the charge transfer bands are also listed in Tables 3.1 and 3.2. For those compounds labeled N/A, no charge transfer bands could be detected. The nonexistence of the bands most likely arises from impurities that serve as quenching centers in the samples. The ratio of heights correlated fairly well to the ratio of areas, decreasing as the integrated area decreased.

Luminescence spectra for the Eu^{+3}-doped Y_2O_3, $BaNaB_9O_{15}$, and $Sr_6YAl(BO_3)_6$, are given in Figure 3.2. As seen, the intensities of the peaks are quite distinct in each case. The band widths are also significantly wider for the hosts $BaNaB_9O_{15}$ and $Sr_6YAl(BO_3)_6$ (15 nm and 20 nm, respectively) in comparison to those of Y_2O_3 (5 nm). The widths associated with the Sr, Y compound most likely derives from the aforementioned distribution of Eu^{+3} over both the Sr and Y sites. Indeed, doubled emission peaks are observed. This distribution also gives rise to a large inhomogeneous broadening. A similar broadening may be expected for the Ba, Na compound where the charge compensating ion K^+ is introduced. Additional thermal quenching, quantum efficiency, and lifetime measurements are planned for those materials having significant red-to-orange rati

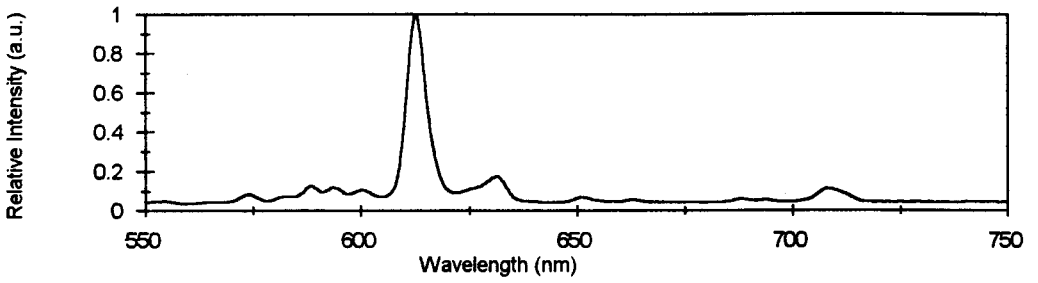

Y_2O_3: 1% Eu^{+3}

λ_{excit}= 394 nm

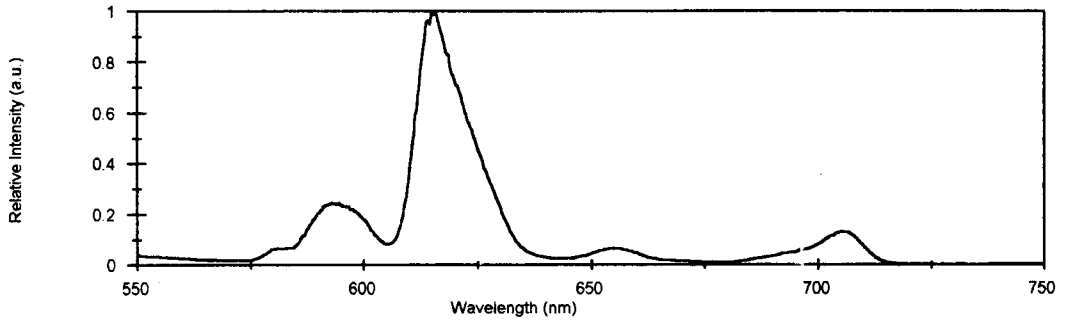

$BaNaB_9O_{15}$: 1% Eu^{+3}

λ_{excit}= 394 nm

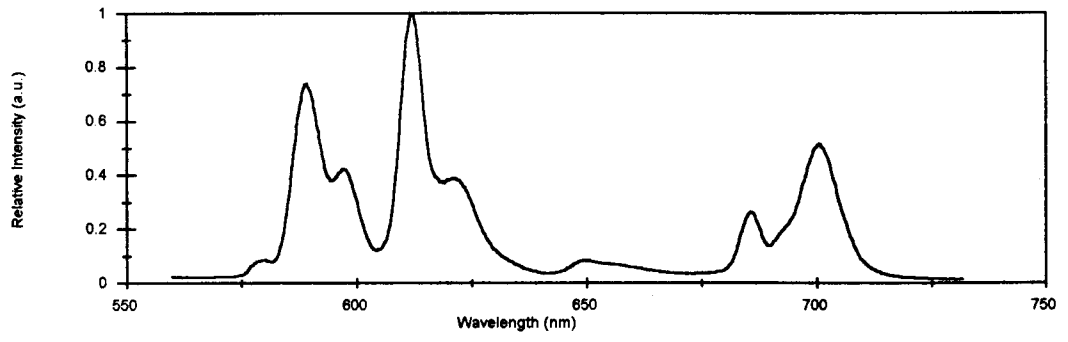

$Sr_6YAl(BO_3)_6$: 1% Eu^{+3}

λ_{excit}= 381 nm

Figure 3.2 Comparison of Emission Spectra of Selected Red Phosphors

References

1. R.B. Hunt Jr., and R.G. Pappalardo, *J. Luminescence* **34**, 134 (1985).

2. K.C. Mishra, P.C. Schmidt, K.H. Johnson, B. G. DeBoer, J.K. Berkowitz and E.A. Dale Phys Rev. B **45**, 45 (1992).

3. B.M.J. Smets, *Mat. Chem. Physics* **16**, 287 (1987).

4. G. Blasse, A. Bril and J.A. De Poorter, *J. Chem. Physics* **53**, 4450 (1970).

5. John B. Gruber, *J. Chem. Physics* **82**, 5374, (1985).

6. R. B.Hunt, and R.G. Pappalardo, *J. Luminescence* **34**, 135, (1985).

7. A. Akella, Ph.D. Dissertation, Oregon State University, (1994).

8. J. Fayos, R.S. Howies and F.P. Glasser, *Acta Cryst* **C41** 1394 (1985).

9. A. Akella and D.A. Keszler, *Main Group Metal Chemistry*, in press.

10. K.I. Schaffers, P.D. Thompson, T. Alekel, J.R. Cox, and D.A. Keszler, *Chem Mater.*, in press.

Chapter 4

Tb^{+3}, Ce^{+3} Luminescence in $SrLiB_9O_{15}$

Abstract

$SrLiB_9O_{15}$ was doped individually with 2% Ce^{+3}, K^+; 1 % Tb^{+3}, K^+; and then co-doped with 1% Tb^{+3}, .25% Ce^{+3}, K^+. The Ce^{+3} sample luminesced violet and had a maximum excitation of 314 nm and a maximum emission of 384 nm. The Tb^{+3} sample luminesced green and had a maximum excitation of 364 nm and a maximum emission of 544 nm. The co-doped sample showed a maximum absorption at 296 nm and a maximum emission at 544 nm; it luminesced a brilliant green.

Introduction

With the increase in sales of color monitors and color televisions, comes the rush by companies to provide the best stereo sound, large screen size, and "true life" color rendition. Fluorescent lamps also require a high color rendition to provide natural lighting. This color representation is produced by three colors: red, blue, and green. Red is provided by Eu^{+3}, blue by Ce^{+3} or Eu^{+2}, and green by Tb^{+3} doped compounds. In the case of fluorescent lamps, the phosphor must be able to efficiently convert 254-nm radiation produced by mercury discharge.

Some factors affecting the choice of a suitable factor are cost, color rendition, quantum efficiency, and high color temperature.

The focus of this experiment is co-doped Tb. Since Tb^{+3} does not have f-d absorption bands that correspond very well with the 254 nm radiation of mercury emission, it must be co-doped with Ce^{+3} to provide a greater effective absorption.[1] This sensitized luminescence allows the Ce^{+3} to act as a sensitizer and transfer energy to the Tb^{+3}, acting as an activator, which then luminesces. This energy is transferred by a nonradiative cascade mechanism when the emission band of the sensitizer overlaps with a strong absorption band of the activator.[2]

The compound $SrLiB_9O_{15}$ was discovered in this lab by K.I. Schaffers, and it has been studied as a possible optical frequency converter.[3] We decided to codope the material with Ce^{+3} and Tb^{+3} to examine if efficient energy transfer from the Ce^{+3} to Tb^{+3} ion could occur. Because of the rigidity of the borate framework and an expected weak crystal field at the Sr^{+2} dopant site, a high-energy emission that overlapped Tb^{+3} absorption peaks was expected. The expectation has been borne out by experiment.

Experimental

Powder samples of $SrLiB_9O_{15}$, doped with 2% Ce^{+3}, K^+; 1% Tb^{+3}, K^+; and 1% Tb^{+3}, 0.25% Ce^{+3}, 1.25% K^+, respectively , were prepared by grinding under hexane, a stoichiometric ratio of $Sr(NO_3)_2$, $LiNO_3$, KNO_3, Tb_4O_7 (Alfa 99.999%),

CeO_2 (Alfa 99.999%) and B_2O_3. The nitrates were decomposed in a platinum crucible at 923 K for thirty minutes followed by regrinding and heating to 1023 K for 12 hours. The co-doped sample of 1% Tb^{+3}, .25% Ce^{+3}, 1.25% K^+, and the 2% Ce^{+3}, K^+ sample were heated to 1023 under H_2/N_2 reducing atmosphere for 24 hours. The resulting powders were confirmed to be single phase by comparing their diffraction patterns to the known pattern of $SrLiB_9O_{15}$.

Spectral data was obtained by using methods outlined in Chapter 2.

Results and Discussion

The $SrLiB_9O_{15}$ structure is a framework of B_3O_7 groups encircling Sr and Li atoms. The Sr atom is nine coordinate, encompassed by O in a distorted tricapped trigonal prismatic environment. The Ce^{+3} and Tb^{+3} ions were doped into this site; its symmetry is C_3.[4]

The individually doped Ce^{+3} sample (Figure 4.1) luminesces a deep violet. The spectrum exhibits an absorption maximum of 314 nm and an emission of 384 nm. The Stokes shift is 5.8 x 10^3 cm^{-1}. Contrary to some Ce^{+3} doped compounds, the emission shows only one peak, indicative of an emissive transition taking place to the $^7F_{5/2}$ level. The $^7F_{7/2}$ level may be distinguishable at a lower temperature.[5]

The individually doped Tb^{+3} sample (Figure 4.2) luminesces a dull green. The spectrum exhibits an absorption maximum of 367 nm and an emission of 547 nm. The emission spectrum shows six peaks, all of the $^5D_4 \rightarrow {}^7F_j$ type

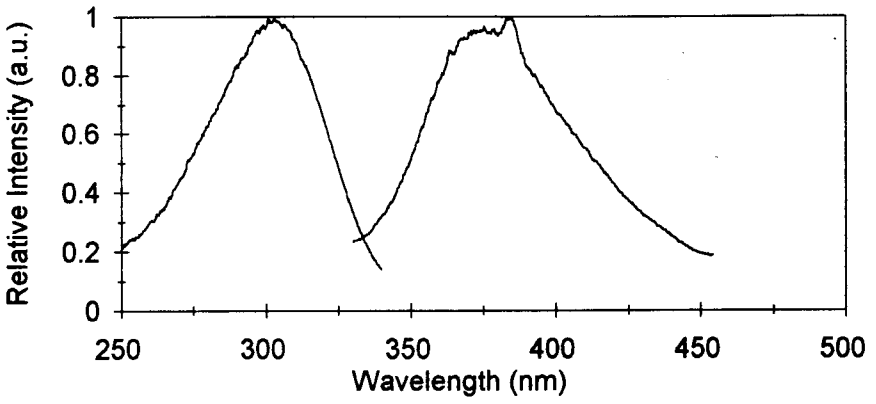

$\lambda_{exc.\ max}$= 314 nm
$\lambda_{em.\ max}$= 384 nm

Figure 4.1 Luminescence Spectra of $SrLiB_9O_{15}$: 1% Ce^{+3}, 1% K^+

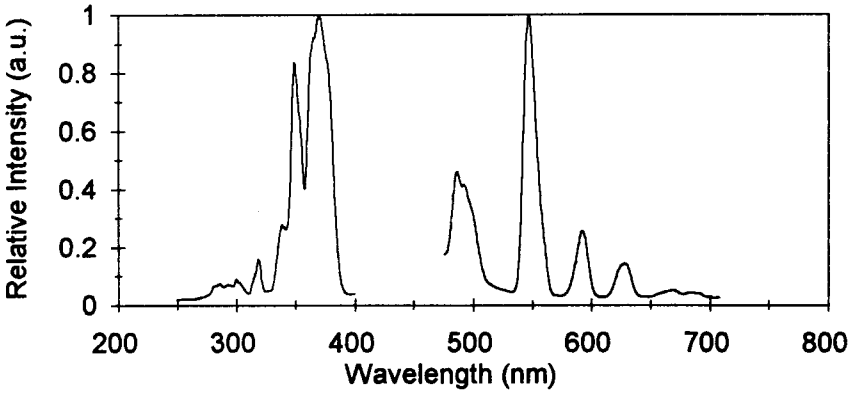

$\lambda_{exc.\ max}$= 367 nm
$\lambda_{em.\ max}$= 547 nm

Figure 4.2 Luminescence Spectra of $SrLiB_9O_{15}$: 1% Tb^{+3}, 1% K^+

transition. Missing is the $^5D_4 \rightarrow {}^7F_2$ transition. The excitation spectrum shows the $^7F_6 \rightarrow {}^5D_2$ transition at 349 nm. The transitions of $^7F_6 \rightarrow {}^5D_3$ and $^7F_6 \rightarrow {}^5L_{10}$ appear to be overlapped in the peak at 367 nm.

As stated previously, in order for energy transfer from Ce^{+3} to Tb^{+3} to take place efficiently, the emission band of the Ce^{+3} ion must overlap the excitation lines of the Tb^{+3} ions. In the case of $SrLiB_9O_{15}$, efficient energy transfer is expected because of the substantial overlap of the emission of Ce^{+3} and the excitation of Tb^{+3} (Figure 4.3). The spectrum of the co-doped sample exhibits an excitation maximum at 296 nm and an emission maximum at 544 nm (Figure 4.4); it luminesces a brilliant green. The spectrum is consistent with complete transfer of energy, as no Ce^{+3} emission is observed. Additional tests of quantum efficiency and concentration-dependent studies are required to determine the true efficacy of this process.

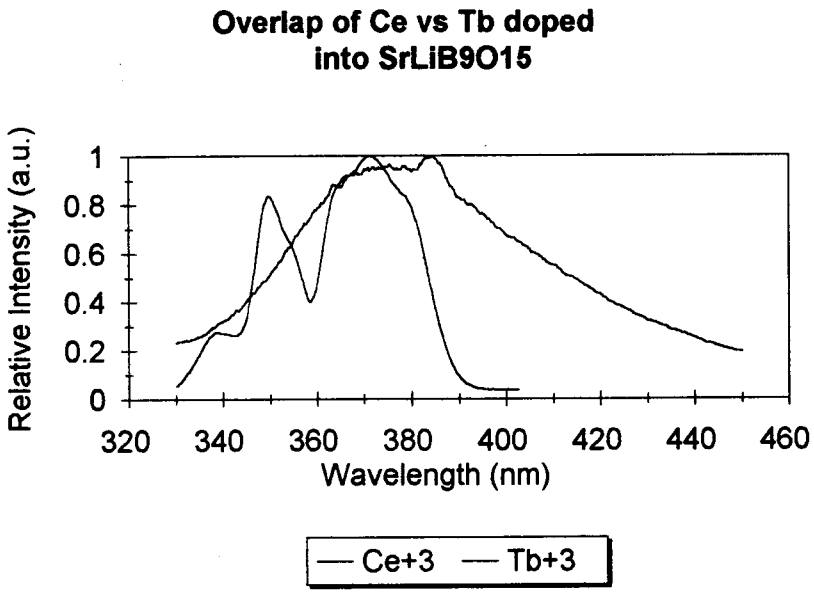

Figure 4.3 Overlap of Ce vs Tb Doped into $SrLiB_9O_{15}$

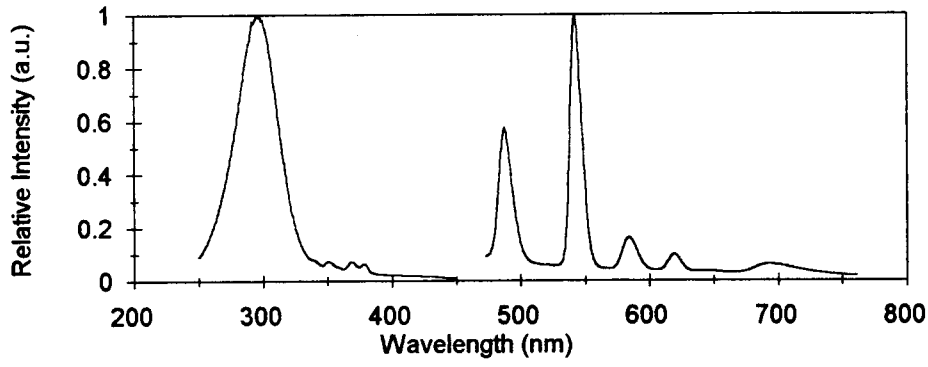

$\lambda_{exc.\ max} = 296$ nm

$\lambda_{em.\ max} = 544$ nm

Figure 4.4 Luminescence Spectra of $SrLiB_9O_{15}$: 1% Tb^{+3}, .25% Ce^{+3}, 1.25 % K^{+}

References

1. T. Welker, *J. Lumin.* **48-49**, 52 (1991).

2. P. Goldberg, ed., Luminescence of Inorganic Solids, 102 (1966).

3. K. I. Schaffers, Ph.D. Dissertation, Oregon State University (1993).

4. K. I. Schaffers, ibid, 85.

5. G. Blasse and A. Bril, *Phil. Tech. Rev.* **31**, 307 (1970).

Chapter 5

Investigation of a Possible Photoionization Effect in $Sr_3In(BO_3)$

Abstract

$Sr_3Sc(BO_3)_3$, $Sr_3In(BO_3)_3$, and $Sr_3Lu(BO_3)_3$ were doped with 0.5 mol % Bi_2O_3 and their luminescence spectra were obtained to investigate a photoionization effect that has been associated with In compounds. This photoionization effect is characterized by calculating the Stokes shift of the compound. The Stokes shifts were calculated for the compounds listed above and were found to be 9.7 x 10^3 cm^{-1}, 2.8 x 10^3 cm^{-1}, 10 x 10^3 cm^{-1}, respectively.

Introduction

Recently Blasse, de Mello Denega, Berezovskaya, and Dotsenko reported emission characteristics for $InBO_3$: Bi^{+3} that differed dramatically from those of $ScBO_3$: Bi^{+3} and $LuBO_3$: Bi^{+3} [1], even though all three compounds are isostructural[2] and the size of the octahedral In dopant site is intermediate to those of $ScBO_3$ and $LuBO_3$-- 86 pm for Lu, 80 pm for In, and 75 pm for Sc.

One of the more dramatic characteristics associated with the material and $InBO_3$: Bi^{+3} is a Stokes shift that is approximately five times greater than those observed for the Sc and Lu derivatives. To account for this behavior, it has been proposed that the excited state electron density at the Bi^{+3} ion is delocalized into

the In-centered 5s5p conduction band on $InBO_3$. The absorption edge of $InBO_3$ is at 220 nm, lower in energy than the 160-nm absorption edges of $ScBO_3$ and $LuBO_3$ that are associated with the intrinsic absorption of the BO_3 group. These edges compare with the absorption of the Bi^{+3} ion which occurs near 275 nm in these hosts. Because there is a significant energy mismatch between the absorption band of Bi^{+3} and the 5s5p conduction band, we wondered if an isolated In site, having higher energy 5s and 5p orbitals, could produce a similar effect. For this reason, we have studied the luminescence properties of Bi^{+3} - doped samples of the compounds $Sr_3Sc(BO_3)_3$, $Sr_3In(BO_3)_3$, and $Sr_3Lu(BO_3)_3$. While the limited data presented here does not allow definitive conclusions with respect to Bi^{+3} and the proposed delocalization model, the host $Sr_3In(BO_3)_3$ does appear to differ from the materials $Sr_3Sc(BO_3)_3$ and $Sr_3Lu(BO_3)_3$.

Experimental

Powder samples of Bi^{+3}-doped $Sr_3Lu(BO_3)_6$ and $Sr_3Sc(BO_3)_3$ were prepared by standard high temperature solid state methods. Stoichiometric quantities of $Sr(NO_3)_2$, Sc_2O_3, Bi_2O_3, and a 3 mol % excess of B_2O_3 were ground under hexane until uniform. The nitrates were decomposed in a platinum crucible, at 973 K for 30 min, followed by regrinding and heating to 1340 K for 12 h. The resulting powders were confirmed to be single phase by analysis of their X-ray diffraction patterns.

The powder sample of $Sr_3In(BO_3)_3$: Bi^{+3} was prepared by using a precursor method. Stoichiometric amounts of Bi_2O_3 and In_2O_3 were dissolved in HCl acid and then precipitated by using NH_4OH (aq). The precipitate was washed and dried at 400 K for 30 min. The resulting solid was ground under hexane with a stoichiometric quantity of $SrCO_3$ and a 5 mol % excess of B_2O_3. The sample was heated at 873 K in a platinum crucible for 2 h, followed by regrinding and heating to 1073 K for 1 h. The compound was heated and reground every 30 minutes with step-wise temperature increases to 1340 K. The compound was then left at 1340 K for 48 h. The resulting compound was confirmed to be single phase by analysis of its diffraction pattern. The concentration of Bi^{+3} was kept below 1.0 mol % to prevent concentration quenching.

Results and Discussion

The compound $Sr_3Sc(BO_3)_3$: Bi^{+3} exhibits an excitation maximum at 330 nm (Figure 5.1) and two emission peaks overlapped with maxima at 408 and 487 nm. Stokes shifts of 6000 and 10,000 cm^{-1} respectively, are observed. The smaller Stokes shift is comparable to that observed in $Sr_6YAl(BO_3)_6$: Bi^{+3} and is consistent with substitution of Bi^{+3} on the Sr site. The low-energy position of the excitation maximum is also consistent with this assertion. The lower energy peak may arise from Bi^{+3} clustering. Pairs and clusters of Bi^{+3} ions have been identified in other hosts. Because their excited-state levels are lower in energy

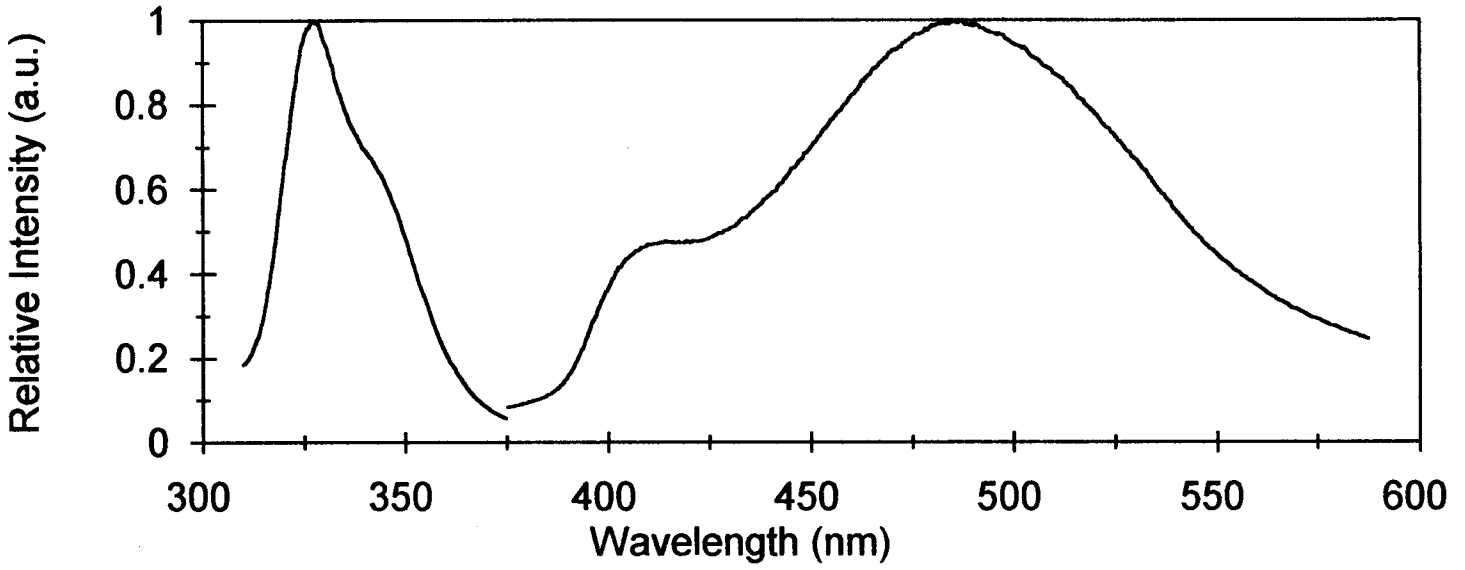

$\lambda_{exc.\ max}$= 330 nm

$\lambda_{em.\ max}$= 487 nm

Figure 5.1 Luminescence Spectra of $Sr_3Sc(BO_3)_3$: 0.5% Bi^{+3}

than those of the isolated ion,[4] their emission peaks occur at longer wavelengths. This clustering has been proposed for $LaBO_3$: Bi^{+3} where emissions observed from two Bi^{+3} sites even though only one crystallographic type of La dopant site is present in the material.[5] Lifetime measurements could be used to differentiate the two types of emission centers. In addition, any emission arising from a clustering of Bi^{+3} should exhibit a concentration dependence.

The compound $Sr_3Lu(BO_3)_3$: Bi^{+3} exhibits an excitation maximum at 329 nm, and like its Sc counterpart it has an emission that appears as two overlapped peaks (Figure 5.2). The emission maxima are at 410 and 499 nm, giving Stokes shifts of 6000 and 10,000 cm^{-1} respectively. Again, the first peak is consistent with both $Sr_3Sc(BO_3)_3$: Bi^{+3} and $Sr_6YAl(BO_3)_3$: Bi^{+3}, although the fine structure here is puzzling.

The compound $Sr_3In(BO_3)_3$: Bi^{+3} exhibits a maximum excitation at 302 nm and a maximum emission at 331 nm (Figure 5.3); the Stokes shift is 2900 cm^{-1}. This result differs substantially from those of the previous two compounds (which are isostructural to $Sr_3In(BO_3)_3$, and it is difficult to rationalize on the basis of the systematic characteristics of Bi^{+3} emission (See Table 5.1). The small Stokes shift is consistent with the placement of the Bi^{+3} ion on the small In^{+3} site, but the position of the excitation maximum is consistent with Bi^{+3} on the larger Sr^{+2} site. Clearly, additional experiments are required to unravel the emission characteristics of Bi^{+3} in these hosts. The preparative procedures, especially the precursor method, should be examined in detail. The full nature of the

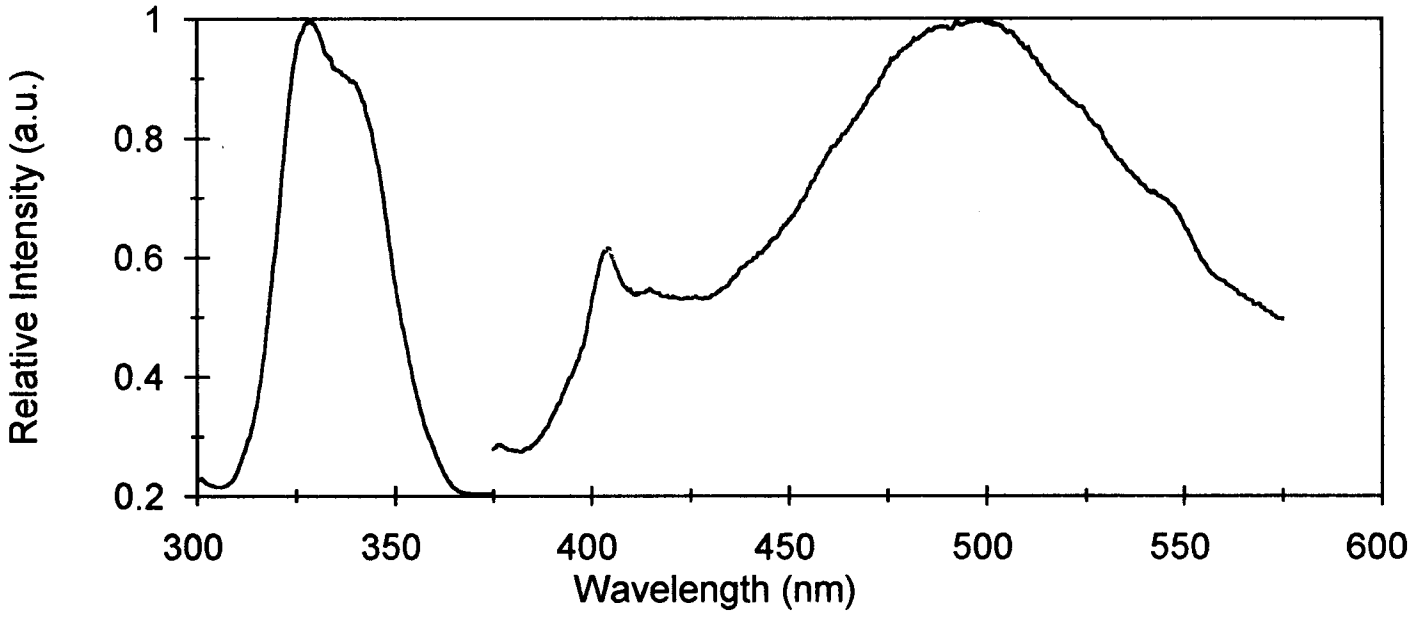

$\lambda_{exc.\ max}$= 329 nm

$\lambda_{em.\ max}$= 499 nm

Figure 5.2 Luminescence Spectra of $Sr_3Lu(BO_3)_3$: 0.5% Bi^{+3}

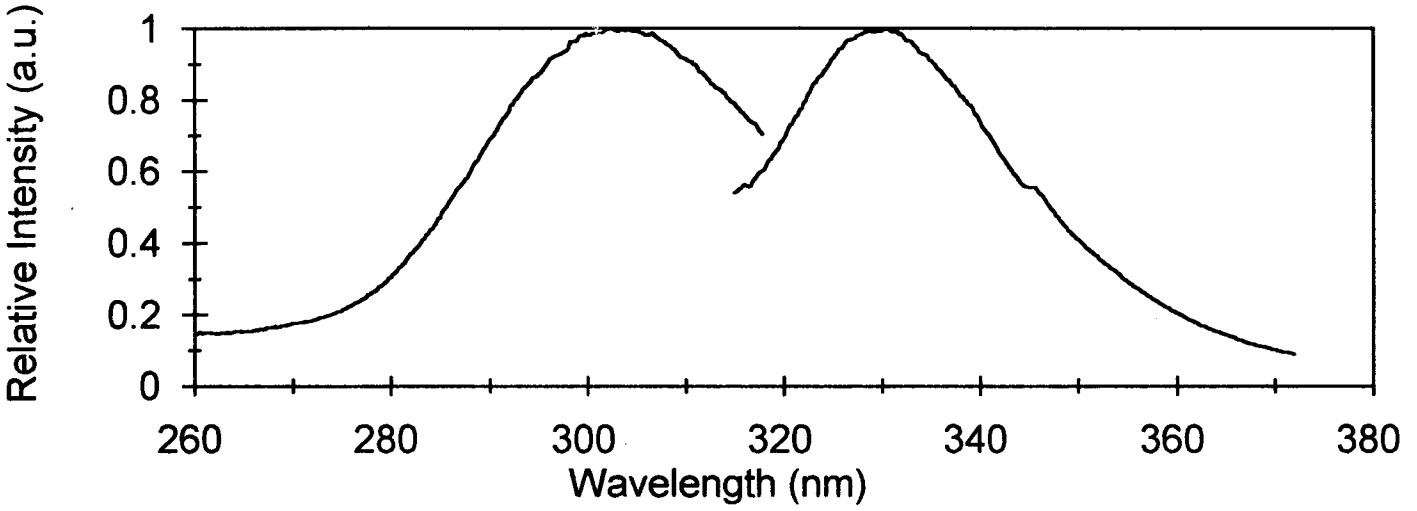

$\lambda_{exc.\ max}$= 302 nm

$\lambda_{em.\ max}$= 331 nm

Figure 5.3 Luminescence Spectra of $Sr_3In(BO_3)_3$: 0.5% Bi^{+3}

COMPOUND	MAXIMUM EXCITATION (nm)	MAXIMUM EMISSION (nm)	STOKES SHIFT ($x 10^3 cm^{-1}$)	REFERENCE
$Sr_3Sc(BO_3)_3$: Bi^{+3}	330	487	10	This work
$Sr_3In(BO_3)_3$: Bi^{+3}	302	331	3	This work
$Sr_3Lu(BO_3)_3$: Bi^{+3}	329	499	10	This work
$Sr_6YAl(BO_3)_6$: Bi^{+3}	314	424	8	This work
$ScBO_3$: Bi^{+3}	285	300	2	1
$LuBO_3$: Bi^{+3}	287	305	2	4
$InBO_3$: Bi^{+3}	280	400	11	4

Table 5.1 Compilation of Excitation and Emission Maxima for Bi^{+3} Compounds.

emitting centers can likely be deduced by performing concentration-dependent studies in connection with measurement of lifetimes and low-temperature spectra.

References

1. G. Blasse,C. de Mello Denega, I. Berezovskaya, and V. Dotsenko, *Sol St Comm.* **91**, 29-31 (1994).

2. J. Cox, Ph. D. Thesis, Oregon State University, 1993.

3. A Wolfert, E.W.J.L. Oomen, and G. Blasse, *J Sol St Chem* **59**, 287 (1985).

4. H.G. Brittain, *J Sol St Chem*, **59** 183 (1985).

5. A Wolfert, E.W.J.L. Oomen, and G. Blasse, *J Luminescence* **31 & 32** , 309 (1985).

Bibliography

Akella, A., Ph.D. Dissertation, Oregon State University, (1994).

Akella, A. and Keszler, D.A., *Main Group Metal Chemistry*, in press.

Andrews, L.J., Beall, G.H. and Lempicki, A., *J. Luminescence*, **36**, 1986, 65.

Blasse, G., *Mat. Chem. Phys.* **16**, 1987, 201.

Blasse, G., *Chem. Mat.* **1**, 1989, 298.

Blasse, G. and Bril, A., *J Chem Phys* **47**, 5140 (1967).

Blasse, G. and Bril, A., *J Chem Phys* **47**, #6, 1921 (1967).

Blasse, G. and Bril, A., *Phil. Tech. Rev.* **31**, 307 (1970).

Blasse, G. and Bril, A., *Progress Solid State Chem.* **18**, 79 (1988).

Blasse, G., Bril, A. and De Poorter, J.A., *J. Chem. Physics* **53**, 4450 (1970).

Blasse, G., de Mello Denega, Berezovskaya, C., I., and Dotsenko, V., *Solid State Comm.* **91**, 29-31 (1994).

Brittain, H.G., *J Sol St Chem*, **59** 183 (1985).

Cox, J., Ph. D. Thesis, Oregon State University, 1993.

Crawford, M. K. and Brixner, L.H., *J. Luminescence*, **48 & 49**, 1991, 37.

DiBartolo, B., ed., Radiationless Processes, Plenum Press, NY, 287 (1980).

Fayos, J., Howies, R.S. and Glasser, F.P., *Acta Cryst* **C41** 1394 (1985).

Fonda, G. R. and Apple, E. F., *Luminescent Materials*, Encyclopedia of Chemical Technology, **14**, 1981, 527.

Goldberg, P., ed., Luminescence of Inorganic Solids, 102 (1966).

Gruber, John B., *J. Chem. Physics* **82**, 5374, (1985).

Hunt, R.B. Jr. and Pappalardo, R.G., *J. Luminescence* **34**, 134,135 (1985).

Mishra, K.C., Schmidt, P.C., Johnson, K.H., DeBoer, B. G., Berkowitz, J.K. and Dale, E.A., Phys Rev. B **45**, 45 (1992).

Schaffers, K. I., Ph.D. Dissertation, Oregon State University (1993).

Schaffers, K.I., Thompson, P.D., Alekel, T., Cox, J.R., and Keszler, D.A., *Chem Mater.*, in press.

Schipper, W.J., van der Voort, D., van den Berg, P., Vroon, Z.A.E.P. and Blasse, G., *Mat Chem Phys* **33**, 312 (1993).

Smets, B.M.J., *Mat. Chem. Physics* **16**, 284, 287 (1987).

Takahashi, K., Miyahara, J. and Shibajara, Y., *J. Electrochem. Soc.*, **132**, 1985, 1492.

Thompson, P.D. and Keszler, D.A., Chem. Mater. 1, 292, (1989).

Timmermans, C.W.M., and Blasse, G., *Solid State Chem* **52**, 228 (1984).

Welker, T., *J. Luminescence*, **48 & 49**, 49-53 (1991).

Wolfert, A., Oomen, E.W.J.L. and Blasse, G., *J Luminescence* **31 & 32**, 308, 309 (1984).

Wolfert, A, Oomen, E.W.J.L., and Blasse, G., *J Sol St Chem* **59**, 287 (1985).

Yamamoto, H. and Matsukiyo, H., J. Luminescence, 48 & 49, 1991, 44.